

Equilibrium Isotherms of Water and Ethanol Vapors on Immobilized Starch Sorbents

Yu-Wei Liu,[†] Tiffany Tang,[†] Tsair-Wang Chung,^{*,†} Charming Huang,[‡] and Yung-Sen Lin[§]

Department of Chemical Engineering/R&D Center for Membrane Technology, Chung Yuan Christian University, Chungli, Taoyuan 320, Taiwan, Department of Environmental Engineering, Kun Shan University, Tainan 710, Taiwan, and Department of Chemical Engineering, Feng Chia University, Taichung 407, Taiwan

In gasohol, the concentration of aqueous ethanol should be further increased from 95.6 % (by mass) to 99.5 % (by mass) by dehydration. In industrial processes, zeolite 3A is usually applied for alcohol–water separation. However, it adsorbs ethanol and water at a similar level (uptake of water/uptake of ethanol = 2.01), resulting in inefficient separation. In this study, potato starch was chosen as an adsorption material because of its very high selectivity and greater capacity for water (uptake of water/uptake of ethanol = 64.18). Conversely, the adsorption capacity of potato starch after regeneration will be substantially reduced, requiring further modification of the material. After regeneration, the unmodified starch decreased its adsorption capacity by 19.70 %, while the immobilized starch had a slight decrease of only 0.56 %. The sol–gel process was used to immobilize the starch, and the equilibrium adsorption isotherm was obtained to describe the immobilized sorbent. The selectivity of the immobilized starch sorbent had a ratio of 4.39 (water to ethanol). Compared to the zeolite 3A in the industrial dehydration process, this selectivity of immobilized starch is almost double that of zeolite 3A. The Langmuir model best describes the experimental isotherm curve of the selected sorbents.

Introduction

In industry, a simple fermentation process can produce an approximately 10 % (by mass) ethanol solution which can be increased to 50 % (by mass) after one distillation. Since water and ethanol will become an azeotropic mixture during distillation, it makes them difficult to separate by simple distillation. Continued effort to produce a more concentrated ethanol by the distillation process will only waste energy and is considered not cost-effective. There are three methods currently used to dehydrate alcohol: azeotropic distillation with an entrainer,¹ membrane distillation,² and the use of adsorbents.³ This research focused on the adsorption method and a proper choice and improvement of the adsorbent. The commonly used material to adsorb water from ethanol is zeolite 3A because of its pore size that lies between the molecular size of water and ethanol.⁴ Although zeolite 3A is fit for ethanol dehydration, its regeneration by degassing at high temperature wastes a lot of energy. Here, we tried to find a new material to replace zeolite 3A with the primary standard of being green and cost-effective. Some studies suggest that bioadsorbents are good materials for the selective removal of water from ethanol.⁵ It was found that potato starch has the best selectivity between water and ethanol,⁶ as compared to other bioadsorbents like cellulose,⁷ cassava starch, and corn starch. However, because of aggregation and gelatinization problems, the capability of potato starch to adsorb water after regeneration will substantially decline.

There are two types of water inside starch particles: free water, which can be found inside the pores, and bonding water,

which interacts with the starch molecules. Starch adsorbs water with limited swelling; it can adsorb water up to half its volume, and it can expand to a volume that ranges from 30 % to 100 % its original size. Regeneration of starch requires degassing at high temperatures. However, the structure of starch will be destroyed when subjected to heat leading to gelatinization and, thus, to irreversible expansion.⁸ For this reason, starch was improved by immobilization in this study. The expansion limit of starch will be controlled by the immobilization matrix. With this, aggregation of starch will be avoided as well as gelatinization. In this research, the enzyme immobilization process was applied to immobilize starch. Immobilization can be reversible or irreversible. The reversible methods include adsorption,⁹ ionic binding,¹⁰ affinity binding,¹¹ chelation,¹² or metal binding and disulfide bonds; irreversible methods include covalent binding,^{13,14} entrapment,^{15,16} microencapsulation,^{17,18} and cross-linking.¹⁹ Irreversible immobilization is the permanent attachment of the enzyme to the support and any means of detaching the enzyme would destroy either the enzyme or the support. This research dealt with sol–gel techniques to encapsulate the starch.

The encapsulation process is based on the entrapment of biomolecules to a matrix. In this process, there is no covalent interaction between the matrix and the starch.^{20,21} Other advantages are the permeability of the matrices and the tunable material porosity. There are two encapsulation methods: sol–gel technology and bioencapsulation in a matrix formed by photocross-linkable polymers.²² The sol–gel process is based on the ability to form metal-oxide, silica, and organosiloxane matrices of defined porosity by the reaction of organic precursors at room temperature.²³ This study aimed to improve the reusability of starch, by immobilizing it using a sol–gel technique, for the successful removal of water from ethanol.

* Corresponding author. E-mail: twchung@cycu.edu.tw. Fax: +886-3-2654199.

[†] Chung Yuan Christian University.

[‡] Kun Shan University.

[§] Feng Chia University.

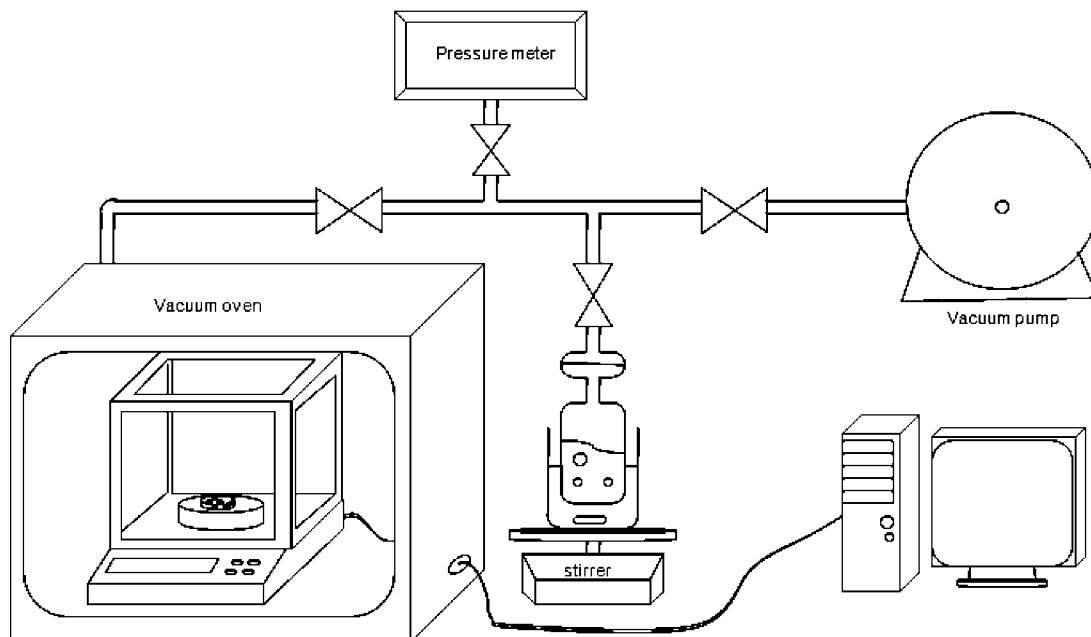


Figure 1. Static adsorption apparatus (gravimetric method) used in this work.

Experimental System

Materials. The reagents used in these experiments include high-purity tetraethyl silicate, $\text{Si}(\text{OC}_2\text{H}_5)_4$, TEOS (Showa, 99 %); hydrochloric acid, HCl (Showa, 35 %); ammonium hydroxide, NH_4OH (Tedia, 29.7 %); and soluble starch with a particle diameter of (30 to 45) μm (Sigma-Aldrich).

Equipment. The surface of the adsorbent was analyzed by a Brunauer–Emmett–Teller (BET) sorptometer (ASAP 2020, Micromeritics). Scanning electronic microscopy (SEM S-3000N-EDX model) was used for the elemental analysis of the hybrid material, while a Hitachi model S-4100 SEM was used for observing the condition of starch on silica. For isotherm adsorption experiments, an equipment schematic is shown in Figure 1.

Starch Immobilization. In the experiment, TEOS was used as a precursor, HCl as a transformation agent, and NH_4OH with deionized water solution as a buffer to adjust the pH of the silica solution. Starch was encapsulated by directly adding it to the mixture. The molar ratio of the sol–gel materials was $\text{TEOS}/\text{H}_2\text{O}/\text{HCl}/\text{NH}_4\text{OH}/\text{starch} = 1:0.02:0.016:[(0.0005 \text{ to } 0.00025) \text{ g} \cdot \text{mol}^{-1} \text{ TEOS}]$. The sol–gel process includes a liquid-phase reaction and gelatinization followed by drying.

Hydrochloric acid was added into a flask containing TEOS and then continuously mixed (600 rpm) at room temperature. After 5 min, the pH was adjusted ($\text{pH} = 2$) by the addition of ammonia alkaline solution with constant stirring for about 1 h. A homogeneous solution indicates completion of the “sol” process; this step involves the hydrolysis of Si-OR to Si-OH . The starch was added directly into the “sol” solution and mixed at 320 rpm to maintain the starch suspension. The mixture was heated at 80 °C to increase the rate of gelatinization; here, Si-OH is converted to Si-O-Si . The gel was then cut into small pieces and oven-dried for about 12 h. The starch to silica ratios (by weight) investigated were different: the ratio of silica and starch in SS-1 was 10:1; SS-2 was 5:1; SS-3 was 2:1; SS-4 was 1:1; and SS-5 was 1:2.

Adsorption Process. Prior to each experiment, the adsorbent was degassed under vacuum at 100 °C for 24 h. Then, it was placed on a microbalance, and the recording of the initial weight was started. The vacuum was started until the required level

Table 1. Surface Properties of the Sorbents (ASAP-2020)

material	BET area surface	micropore volume	average pore diameter
	$\text{m}^2 \cdot \text{g}^{-1}$	$\text{cm}^3 \cdot \text{g}^{-1}$	Å
silica gel	482	0.227	18
SS-1	246	0.117	18
SS-2	246	0.115	18
SS-3	168	0.074	17
SS-4	87	0.035	16
SS-5	74	0.037	19

was reached. The appropriate volume of gas adsorbate was then allowed to pass through the system until the system reached the desired pressure. Pressure and weight recording was started soon after the balance stabilized. The described steps were repeated until the gas adsorbate reached its saturated vapor pressure (Figure 1). Mapping the pressure versus the adsorbed weight gave rise to the equilibrium isotherm curves.

Results and Discussion

BET Surface Analysis. It is shown in Table 1 that, when silica gel was mixed with starch, the porosity of the material decreases. Increasing the ratio of starch in the mixture causes a decrease in both the BET surface area and the average pore diameter except for the SS-5, and the variation of the surface properties of the mixtures is due to the almost nonporous nature of the starch particles.

SEM and Energy-Dispersive X-ray (EDX) Analysis of the Hybrid Material. Under different magnifications, it was observed that the starch was embedded (Figure 2) on the silica gel after immobilization. In hybrid material, more starch was added, and more circular particles inside the silica gel can be found with the same magnification. That means that the circular particles are the starches in the figure (Figure 3). With the same magnification as the SEM-EDX analysis, the elemental analysis of the material shows that the addition of starch increases the carbon content of the resulting material; this confirms the successful immobilization of starch (Table 2). However, under the same unit area, the locations formerly occupied by the silicon particles would be replaced by starch.

When too much starch was added into the silica gel, the amount of silicon in the mixture would not be enough to

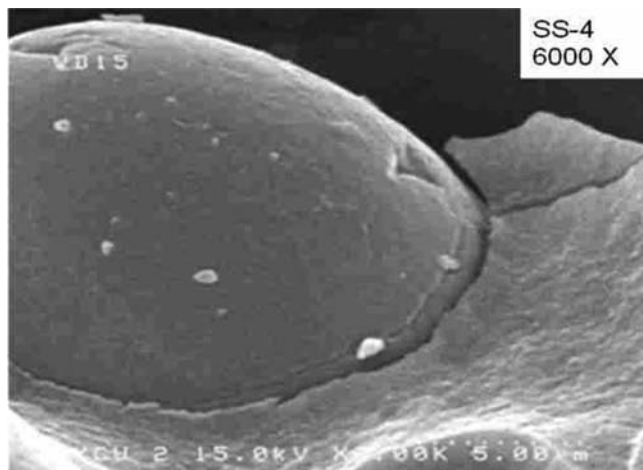


Figure 2. Condition of starch on silica (SEM photo of sorbent SS-4).

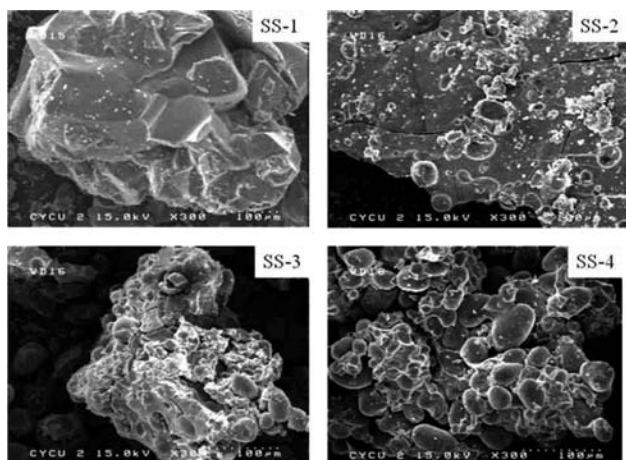


Figure 3. Condition of different amounts of starch immobilized on silica (SEM photo).

immobilize and interact with the starch particles. Instead, the starch particles would interact with each other to form a large mass of starch. The key to higher water to ethanol selectivity of starch is the type of interaction it uses; starch uses hydrogen bonding to capture water molecules, while silica gel uses van der Waals interactions. The highest amount of starch that can be added is a 1:1 (SS-4) ratio with the silica gel. Increasing the starch content further (SS-5) will cause a decrease in the percent (by mass) of the elemental carbon in the mixture.

Selectivity of Water and Ethanol. For water adsorption, potato starch is the best material (Figure 4), while pure silica is the best for ethanol adsorption (Figure 5). Because of the hydrophilic property of silica, it adsorbs both water and ethanol well. However, in terms of water selectivity, potato starch is superior over silica gel (Figure 6).

In order for the starch to be used repeatedly, it needs to be immobilized to a support like silica gel. Increasing the amount of starch in the silica gel increases the selectivity of the material but not as high as the selectivity of the pure starch. The new hybrid sorbent has a selectivity of up to 4.38 (water/ethanol) as compared to the commonly used adsorbent zeolite 3A with a

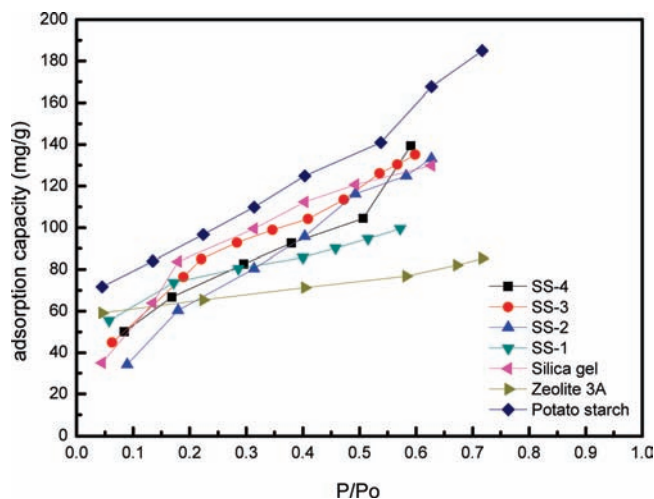


Figure 4. Water vapor equilibrium isotherms for selected sorbents (298 K). P/P_0 is the partial pressure, and P_0/P_0 is the saturated pressure of the sorbate.

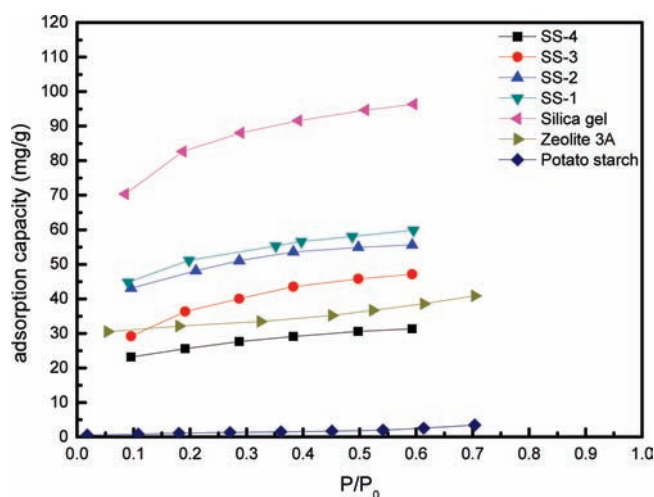


Figure 5. Ethanol vapor equilibrium isotherms for selected sorbents (298 K). P/P_0 is the partial pressure, and P_0/P_0 is the saturated pressure of the sorbate.

selectivity of less than half of that of the new sorbent (Table 3). The regeneration temperature required for the new material is also lower than that of zeolite, making it a potential adsorbent replacement for zeolite 3A.

Original Starch Regeneration Adsorption Test. In raw starch, regeneration adsorption tests gave adsorption reductions of 19.70 % (second test), 26.94 % (third test), and 37.00 % (fourth test), when compared with the first test. The regeneration capacity is not good for the raw starch adsorption test. After four adsorption and regeneration tests the capacity of potato starch had been reduced to sixty percent. This reduction is not good in industry (Figure 7).

SS-3 Regeneration Adsorption Test. The water uptake of the SS-3 mixture after the first regeneration increases by 0.081 % followed by 1.14 % and 5.32 % for the second and third regenerations, respectively (Figure 8). However, for the fourth regeneration, a decrease in water uptake of 0.56 % was observed.

Table 2. Elemental Analysis of the Hybrid Sorbents in This Study

sorbent element	SS-1			SS-2			SS-3			SS-4			SS-5		
	C	O	Si	C	O	Si	C	O	Si	C	O	Si	C	O	Si
% (by mass)	13.78	49.01	37.21	26.94	50.19	22.86	36.13	50.25	13.62	39.16	49.15	11.69	21.37	50.66	27.97
atomic %	20.72	55.34	23.94	36.21	50.65	13.14	45.34	47.35	7.31	48.31	45.52	6.17	29.95	53.29	16.76

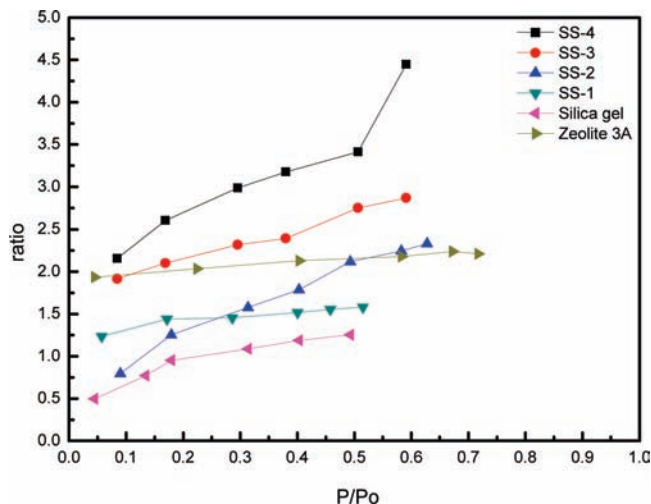


Figure 6. Ratio of water-to-ethanol adsorption in selected sorbents (298 K). P/P_o is the partial pressure, and P_o/P_a is the saturated pressure of the sorbate.

Table 3. Adsorption Ratio of Water-to-Ethanol Vapors

adsorbent	water adsorbed		ethanol adsorbed		ratio (water/ethanol)
	$\text{mg} \cdot \text{g}^{-1}$		$\text{mg} \cdot \text{g}^{-1}$		
SS-4	139.37	31.76	4.39		
SS-3	135.11	47.07	2.87		
SS-2	133.21	57.2	2.33		
SS-1	99.51	59.9	1.66		
pure silica	129.86	95.65	1.36		
zeolite 3A	82.13	40.86	2.01		
potato starch	167.56	2.61	64.18		

The reason for the increasing uptake for the first three regeneration steps is the formation of new pores every regeneration step which increases the surface area of the material. The decrease in water uptake for the fourth regeneration was due to aging. For the first three regenerations, the rate to generate new pores is faster than that of aging, but for the fourth regeneration, the rate of aging is faster than that for new pore formation, resulting in a decrease in adsorption.

SS-4 Regeneration Adsorption Test. For the SS-4 mixture, a reduction of water uptake was observed for the first three regenerations, which were 7.63 %, 9.79 %, and 8.18 %, respectively (Figure 9). As opposed to the result in SS-3, the fourth regeneration results in an increase in water uptake. Since

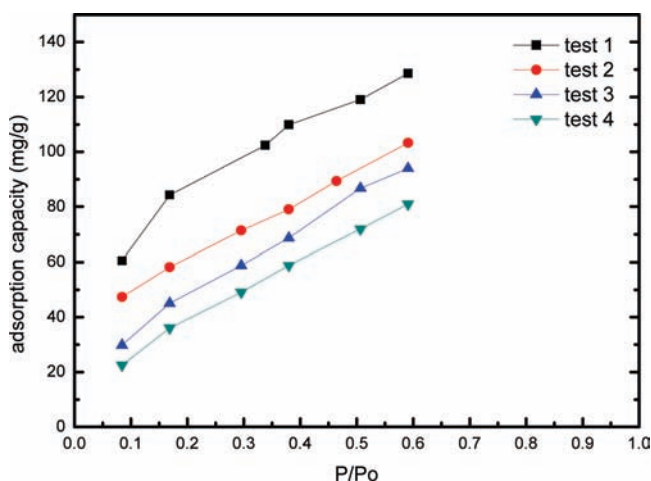


Figure 7. Adsorption capacity variation of the original starch sorbent in different reuse times (298 K). P/P_o is the partial pressure, and P_o/P_a is the saturated pressure of the sorbate.

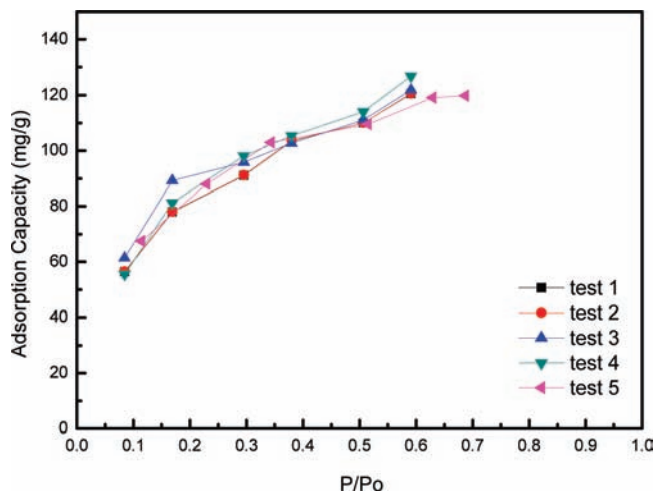


Figure 8. Adsorption capacity variation of sorbent SS-3 in different reuse times (298 K). P/P_o is the partial pressure, and P_o/P_a is the saturated pressure of the sorbate.

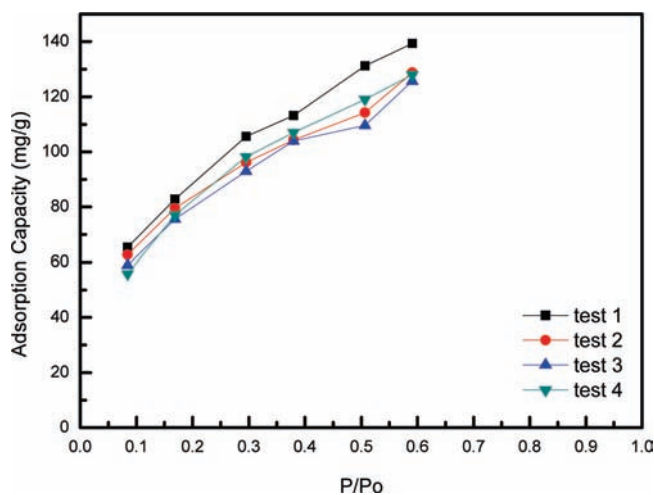


Figure 9. Adsorption capacity variation of sorbent SS-4 in different reuse times (298 K). P/P_o is the partial pressure, and P_o/P_a is the saturated pressure of the sorbate.

the starch content is higher, the rate of aging is faster for the SS-4 hybrid. A continuous increase in the rate of aging surmounts the rate of pore formation, which results in a decrease in water uptake for each regeneration step. After the three regeneration steps, the limit of aging was reached, allowing pore formation to take effect in the fourth regeneration.

Data Regression. The adsorption isotherm fitting for each material was done using the nonlinear least-squares method with the Langmuir and BET models. Using the Langmuir isotherm model for water adsorption, better results were observed for the newly synthesized materials together with zeolite 3A, potato starch, and silicone mixture as shown by the higher R^2 values (Table 4). From the regression data, the maximum single layer adsorption capacity (q_m) for all the immobilized sorbents were between (5 to 15) $\text{mmol} \cdot \text{g}^{-1}$, while those for potato starch, silica gel, and the Si/Al mixture (zeolite) were between (4 to 12) $\text{mmol} \cdot \text{g}^{-1}$. The BET model is not fit to describe the experimental data because it produces unsatisfactory R^2 values and also a meaningless q_m since it is already lower than the experimental data. For ethanol adsorption, the Langmuir model is still better except for zeolite 3A (Table 5). The maximum single layer adsorption capacity (q_m) for ethanol uptake was calculated to be between (1 and 3) $\text{mmol} \cdot \text{g}^{-1}$.

Table 4. Regression Constants of Selected Adsorption Models for Water Vapor Adsorption Data in This Work (298 K)

	model	R^2	q_m	
			$\text{mmol} \cdot \text{g}^{-1}$	b
SS-1	Langmuir	0.998	5.665	17.913
	BET	0.706	0.363	7.185
SS-2	Langmuir	0.999	15.584	1.387
	BET	0.988	0.755	1.158
SS-3	Langmuir	0.997	10.374	3.656
	BET	0.936	0.633	2.081
SS-4	Langmuir	0.987	10.61	2.986
	BET	0.833	0.640	1.742
silica gel	Langmuir	0.999	9.375	5.017
	BET	0.979	0.579	2.797
zeolite 3A	Langmuir	0.995	4.438	54.019
	BET	0.146	0.295	14.427
potato starch	Langmuir	0.981	12.113	4.272
	BET	0.960	3.581	20.226

Table 5. Regression Constants of Selected Adsorption Models for Ethanol Vapor Adsorption Data in This Work (298 K)

	model	R^2	q_m	
			$\text{mmol} \cdot \text{g}^{-1}$	b
SS-1	Langmuir	0.967	1.944	26.964
	BET	0.602	0.125	9.103
SS-2	Langmuir	0.964	1.849	25.413
	BET	0.427	0.124	7.358
SS-3	Langmuir	0.988	1.659	11.982
	BET	0.407	0.794	6.469
SS-4	Langmuir	0.933	1.027	22.207
	BET	0.581	0.067	7.636
silica gel	Langmuir	0.987	3.166	25.531
	BET	0.685	0.204	8.750
zeolite 3A	Langmuir	0.561	1.185	61.614
	BET	0.381	0.054	0.994
potato starch	Langmuir	0.874	0.168	0.008
	BET	0.583	0.100	0.286

Conclusion

On the basis of the experiment, the optimum ratio of starch to silica gel for selective water to ethanol adsorption is 1:1 (w/w). A decrease in water uptake of 37.00 % was observed for the unmodified starch after three regenerations, while a significantly lower decrease in water uptake was observed for the immobilized starch sorbents after the same number of regenerations. The rate of decrease in water uptake for the SS-3 hybrid was lower than that of the SS-4 hybrid because of the amount of starch present. The impact of regeneration on adsorption capability is more pronounced on starch than on silica gel. In terms of the high water to ethanol selectivity, the SS-4 hybrid (with a water to ethanol ratio of 4.39) is better than SS-3. In fitting the regression data for the new materials as well as potato starch and silicone, the Langmuir model provides good R^2 values.

Literature Cited

- (1) Düssel, R.; Stichlmair, J. Separation of Azeotropic Mixture by Batch Distillation using an Entrainer. *Comput. Chem. Eng.* **1995**, *19*, 113–118.
- (2) Lawson, K. W.; Lloyd, D. R. Membrane Distillation (review). *J. Membr. Sci.* **1997**, *124*, 1–25.
- (3) Carmo, M. J.; Gubulin, J. C. Ethanol-Water Adsorption on Commercial 3A Zeolites: Kinetic and Thermodynamic Data. *Braz. J. Chem. Eng.* **1997**, *14*, 125–132.

- (4) Lalik, E.; Mirek, R.; Rakoczy, J.; Groszek, A. Microcalorimetric Study of Sorption of Water and Ethanol in Zeolites 3A and 5A. *Catal. Today* **2006**, *114*, 242–247.
- (5) Czepirski, L.; Czepirska, E. K. Adsorptive Properties of Biobased Adsorbents. *Adsorption* **2005**, *11*, 757–761.
- (6) Wang, K. S.; Liao, C. C.; Chu, R. Q.; Chung, T. W. Equilibrium Isotherms of Water and Ethanol Vapors on Starch Sorbents and Zeolite 3A. *J. Chem. Eng. Data* **2010**, *55*, 3334–3337.
- (7) Quintero, J. A.; Cardona, A. C. Ethanol Dehydration by Adsorption with Starchy and Cellulosic Materials. *Ind. Eng. Chem. Res.* **2009**, *48*, 6783–6788.
- (8) Biliaderis, C. G.; Maurice, T. J.; Vose, J. R. Starch Gelatinization Phenomena Studied by Differential Scanning Calorimetry. *J. Food Sci.* **1980**, *45*, 1669–1674.
- (9) Mateo, C.; Abian, O.; Roberto, F. L.; Guisan, J. M. Reversible Enzyme Immobilization via a Very Strong and Nondistorting Ionic Adsorption on Support-Polyethylenimine Composites. *Biotechnol. Bioeng.* **1999**, *68*, 98–105.
- (10) Tang, Z. M.; Kang, J. W. Enzyme Inhibitor Screening by Capillary Electrophoresis with an on-Column Immobilized Enzyme Microreactor Created by an Ionic Binding Technique. *Anal. Chem.* **2006**, *78*, 2514–2520.
- (11) Pathange, L. P.; Bevan, D. R.; Larson, T. J.; Zhang, C. Correlation between Protein Binding Strength on Immobilized Metal Affinity Chromatography and the Histidine-Related Protein Surface Structure. *Anal. Chem.* **2006**, *78*, 4443–4449.
- (12) Hoorn, H. J.; Joode, P.; Driessen, W. L.; Reedijk, J. Metal-Binding Affinity of a Series of Amino-Alkylbenzimidazoles Immobilized on Silica. *React. Funct. Polym.* **1995**, *27*, 223–235.
- (13) Alkorta, I.; Garbisu, C.; Llama, M. J.; Serra, J. L. Immobilization of Pectin Lyase from *Penicillium Italicum* by Covalent Binding to Nylon. *Enzyme Microb. Technol.* **1996**, *18*, 141–146.
- (14) Wang, P.; Dai, S.; Waezsada, S. D.; Tsao, A. Y.; Davison, B. H. Enzyme Stabilization by Covalent Binding in Nanoporous Sol-Gel Glass for Nonaqueous Biocatalysis. *Biotechnol. Bioeng.* **2001**, *74*, 249–255.
- (15) Reetz, M. T.; Zonta, A.; Simpelkamp, J. Efficient Immobilization of Lipases by Entrapment in Hydrophobic Sol-Gel Materials. *Biotechnol. Bioeng.* **1995**, *49*, 527–534.
- (16) Kim, K. O.; Lim, S. Y.; Hahn, G. H.; Lee, S. H.; Park, C. B.; Kim, D. M. Cell-Free Synthesis of Functional Proteins Using Transcription/Translation Machinery Entrapped in Silica Sol-Gel Matrix. *Biotechnol. Bioeng.* **2008**, *102*, 303–307.
- (17) Mureseanu, M.; Galarneau, A.; Renard, G.; Fajula, F. A New Mesoporous Micelle-Templated Silica Route for Enzyme Encapsulation. *Langmuir* **2005**, *21*, 4648–4655.
- (18) Takimoto, A.; Shiomi, T.; Ino, K.; Tsunoda, T.; Kawai, A.; Mizukami, F.; Sakaguchi, K. Encapsulation of Cellulase with Mesoporous Silica (SBA-15). *Microporous Mesoporous Mater.* **2008**, *116*, 601–606.
- (19) Pollak, A.; Blumenfeld, H.; Wax, M.; Baughn, R. L.; Whitesides, G. M. Enzyme Immobilization by Condensation Copolymerization into Crosslinked Polyacrylamide Gels. *J. Am. Chem. Soc.* **1980**, *102*, 6324–6336.
- (20) Edmiston, P. L.; Wambolt, C. L.; Smith, M. K.; Saavedra, S. S. Spectroscopic Characterization of Albumin and Myoglobin Entrapped in Bulk Sol-gel Glasses. *J. Colloid Interface Sci.* **1994**, *163*, 395–406.
- (21) Dave, B. C.; Soyey, H.; Miller, J. M.; Dunn, B.; Valentine, J. S.; Zink, J. I. Synthesis of Protein-Doped Sol-Gel SiO₂ Thin Films: Evidence for Rotational Mobility of Encapsulated Cytochrome. *Chem. Mater.* **1995**, *7*, 1431–1434.
- (22) Guisan, J. M. *Immobilization of Enzymes and Cells*; Humana Press: Totowa, NJ, 2006.
- (23) Hench, L. L.; West, J. K. The Sol-Gel Process. *Chem. Rev.* **1990**, *90*, 33–72.

Received for review July 25, 2010. Accepted October 30, 2010. This research was supported by a project on specific research fields in Chung Yuan Christian University, Taiwan, under Grant CYCU-98-CR-CE, the National Science Council under Grant NSC98-2221-E-033-028, and the Ministry of Education by the Center of Excellence project.

JE100773S